Ankyrin-B p.S646F undergoes increased proteasome degradation and reduces cell viability in the H9c2 rat ventricular cardiomyoblast cell line

Lena Chen, Catherine S.W. Choi, Juan C. Sanchez-Arias, Laura T. Arbour, Leigh Anne Swayne

This article will be published in Biochemistry and Cell Biology at:

https://www.nrcresearchpress.com/journal/bcb

Ankyrin-B p.S646F undergoes increased proteasome degradation and reduces cell viability in the H9c2 rat ventricular cardiomyoblast cell line

Lena Chen[1†], Catherine S.W. Choi[1†], Juan C. Sanchez-Arias[1], Laura T. Arbour[1,2,3], Leigh Anne Swayne[1,2*]

[1]Divison of Medical Sciences, University of Victoria, Victoria, British Columbia, Canada

[2]Island Medical Program, University of British Columbia, Victoria, British Columbia, Canada

[3]Department of Medical Genetics, University of British Columbia, Victoria, British Columbia, Canada

† These authors have contributed equally to this work

***Correspondence:** Leigh Anne Swayne: lswayne@uvic.ca

ABSTRACT

Ankyrin-B (AnkB) is scaffolding protein that anchors integral membrane proteins to the cardiomyocyte cytoskeleton. We recently identified an AnkB variant, AnkB p.S646F (*ANK2* c.1937 C>T) associated with a phenotype ranging from predisposition for cardiac arrhythmia to cardiomyopathy. AnkB p.S646F exhibited reduced expression levels in the H9c2 rat ventricular-derived cardiomyoblast cell line relative to wildtype AnkB. Here we demonstrate that AnkB is regulated by proteasomal degradation and proteasome inhibition rescues AnkB p.S646F expression levels in H9c2 cells, although this effect is not conserved with differentiation. We also compared the impact of wildtype AnkB and AnkB p.S646F on cell viability and proliferation. AnkB p.S646F expression resulted in decreased cell viability at 30 hours post-transfection, whereas we observed a greater proportion of cycling, Ki67-positive cells at 48 h post-transfection. Notably, the number of GFP-positive cells was low, and was consistent between wildtype AnkB and AnkB p.S646F expressing cells, suggesting that AnkB and AnkB p.S646F affected paracrine communication between H9c2 cells differentially. In summary, this work reveals AnkB levels are regulated by the proteasome, and that AnkB p.S646F compromises cell viability. Together these findings provide key new insights into the putative cellular and molecular mechanisms of AnkB-related cardiac disease.

Key Words: Ankyrin-B, proteasome, cardiomyocytes, cell viability

INTRODUCTION

Ankyrin-B (AnkB) is a large 220 kDa scaffolding protein that plays a critical role in tethering the contractile machinery (i.e. ion channels and transporters) in a specialized region of the cardiomyocyte cell membrane (Mohler et al. 2007b; Koenig and Mohler 2017; El Refaey and Mohler 2017). Variants in the *ANK2* gene can lead to "Ankyrin-B Syndrome" mainly characterized by a predisposition to cardiac arrhythmia and an increased risk of sudden cardiac death (Mohler et al. 2004, 2007b). The phenotype of AnkB$^{+/-}$ mice, partially recapitulated pathologies observed in human *ANK2* gene loss of function variants, such as predisposition to arrhythmia (Mohler et al. 2007a). AnkB knockout mice are postnatal lethal, where AnkB knockout cardiomyocytes display abnormal contraction as well as irregular calcium homeostasis (Scotland et al. 1998; Mohler et al. 2002), which could result from altered development at the cellular and molecular level.

We recently reported a new variant AnkB p.S646F (*ANK2* c.1937 C>T), a mutation in the membrane binding domain (MBD), whose carriers displayed variety of clinical features including long QT syndrome, dilated cardiomyopathy with associated sudden death, congenital heart malformation, Wolff–Parkinson–White syndrome, and seizures (Swayne et al. 2017). AnkB p.S646F is similar to other AnkB variants in that it confers susceptibility to cardiac arrhythmia; however, AnkB p.S646F is also uniquely associated with a broader phenotype including structural abnormalities. This suggests AnkB may play a more prominent role in development and formation of the heart than previously understood. Moreover, changes in AnkB expression levels have been implicated in aberrant cardiomyocyte development (Mohler et al. 2003, 2004; Swayne et al. 2017). Our previous study revealed that expression of AnkB p.S646F was significantly reduced relative to wildtype AnkB (Swayne et al. 2017). Here we investigated

the cellular degradation pathway for AnkB as well as the impact of the AnkB p.S646F variant on cardiomyoblast growth and viability. Our findings shed important new light on AnkB in the context of cardiomyocyte biology and pathophysiology.

METHODS

Cell culture

The H9c2 rat ventricular-derived cardiomyoblast cell line was obtained from the American Type Culture Collection (ATCC CRL-1446). H9c2 cells were cultured in Dulbecco's Modified Eagle Medium (DMEM, ThermoFisher Scientific, Burlington, CA) supplemented with 10% fetal bovine serum (FBS), 100 U/mL penicillin and 100 μg/mL streptomycin at 37 °C in 5% CO_2. Cells were passaged at 70% confluence. H9c2 cells were seeded at 16,667 cells/cm^2 24 h prior to transfection as per manufacturer's protocol (Polyplus-transfection® SA/VWR, Edmonton, CA). The wildtype ankyrin-B-pAcGFP-n1 and mutant ankyrin-B p.S646F-pAcGFP-n1 were created as previously described (Swayne et al. 2017).

H9c2 cells were differentiated as previously described by Ménard *et al.* (Menard et al. 1999). Briefly, H9c2 cells were seeded at 8,333 cells/cm^2 and transfected the next day. One day post-transfection, media was changed to DMEM with 1% FBS, 10 nM all-*trans*-retinoic acid (RA), 100 U/mL penicillin and 100 μg/mL streptomycin (Diff DMEM). Three days post-transfection, media was replaced with Diff DMEM with 500 μg/mL of G418 to maintain heterologous gene expression.

Determination of protein degradation pathway

To determine the degradation pathway, H9c2 cells were treated 6 h post transfection with 0, 25, or 50 nM of the proteasome inhibitor PS-341 (ThermoFisher Scientific, Burlington, CA)

and 0, 10 or 25 nM of the lysosome inhibitor Bafilomycin A (BafA; Millipore Sigma, Oakville, CA) for 12 h until cell lysis for Western blot analysis. To test if AnkB p.S646F levels could be rescued by proteasomal inhibition, H9c2 cells were transfected with either wildtype AnkB or AnkB p.S646F -GFP and treated with 0 or 10 nM PS-341, 6 h after transfection. Cells were lysed 12 h after PS-341 treatment for Western blot analysis. For H9c2 differentiation, cells were collected 5 days post-transfection and were treated with PS-341 for 12 h prior to collection.

Western blotting

Samples were homogenized in RIPA buffer (10 mM PBS [150 mM NaCl, 9.1 mM dibasic sodium phosphate, 1.7 mM monobasic sodium phosphate], 1% IGEPAL, 0.5% sodium deoxycholate, and 0.1% SDS) supplemented with protease inhibitor cocktail at 1 μL/10^6 cells (stock: 0.104 mM 4-(2-aminoethyl)benzenesulfonyl fluoride hydrochloride, 0.08 mM aprotinin, 4 mM bestatin hydrochloride, 1.4 mM N-(trans- epoxysuccinyl)-L-leucine 4-guanidinobutylamide, 2 mM leupeptin hemisulfate salt, and 1.5 mM pepstatin-A; Millipore Sigma, Oakville, CA), PMSF at 2 μL/10^6 cells and 1 mM EDTA, passed through a 27-gauge needle twice, and incubated for 30 minutes on ice. Cell lysates were then centrifuged at 4°C for 20 minutes at 12,000 rpm and supernatant was collected. Lysates were heated for 5 min at 95 °C under reducing conditions (dithiothreitol (DTT) and β-mercaptoethanol), separated by SDS-PAGE and transferred to 0.2 μm pore PVDF membrane (Bio-Rad, Missasauga, CA). The membrane was blocked with 5% non-fat milk in PBST or TBST and then incubated with indicated antibodies in the blocking solution. Primary antibodies used include anti-GFP (1:8000 – 1:128000; ThermoFisher Scientific, Burlington, CA), anti-β-actin (1:8000 – 1:128000), anti-AnkB (1:500; ThermoFisher Scientific, Burlington, CA). Secondary antibodies were horseradish peroxidase (HRP)-conjugated AffiniPure donkey anti-rabbit IgG (1:2000), HRP-conjugated

AffiniPure donkey anti-mouse IgG (1:4000 – 1:8000; both from Jackson ImmunoResearch, West Grove Pennsylvania, USA). Bands were visualized with Clarity Western enhanced chemiluminescence substrate (Bio-Rad, Missasauga, CA.) and quantified by densitometry analysis with Image J (Version 1.45) (Schneider et al. 2012).

Immunocytochemistry and Confocal Microscopy

H9c2 cells were seeded onto poly-D-lysine laminin coated coverslips (NeuroVitro, Vancouver, USA) at 8,333 cells/cm^2 and transfected 24 h post seeding. Forty-eight hours post-transfection, coverslips were fixed for 10 minutes with warmed 4% PFA supplemented with 4% sucrose, followed by 3 washes with PBS and stored in PBS at 4°C until used. A subset of coverslips was washed with PBS and incubated with Wheat Germ Agglutinin (WGA) Alexa Fluor™ 647-conjugate (W32466, Thermo-Fisher) in 1X HBSS (14185052, Thermo-Fisher) for 5 minutes, washed 3 times in PBS, fixed with 4% PFA and 4% sucrose, and then stored at 4^{o}C until used. For immunocytochemistry, cells on coverslips were permeabilized with 0.25% Triton-X for 10 minutes, blocked with 10% donkey serum (DS, Jackson ImmunoResearch), 1% BSA, and glycine (22.52 mg/mL) in PBST for 30 minutes at room temperature. Following blocking, coverslips were incubated overnight at 4°C with primary antibodies, anti-Ki67 (1:200, BD Pharmingen, San Jose, CA) and anti-AnkB (1:200), diluted in 1% BSA, and 5% DS in PBST (antibody buffer), washed three times in PBS (10 minutes each), and incubated with secondary antibody, AlexaFluor 586-conjugated donkey anti-mouse IgG (1:600; A10037, Thermo-Fisher), in antibody buffer. Acti-stain 670 phalloidin (PHDN1-A, Cytoskeleton, Inc) was used for coverslips not labelled with WGA. Qualitative determination of AnkB-GFP and AnkB p.S646F -GFP localization was done by acquiring high resolution confocal images (2048 x 2048, pixel size: 0.142 μm) using a Leica TSC SP8 microscope and a 40X oil-immersion objective (1.40

NA, pinhole 1.0 AU). For Ki67+ nuclei quantification, high resolution images (2048 x 2048, pixel size: 0.568 μm) were acquired using a 10X dry-objective (0.3 NA, pinhole: 4 AU). Analysis of Ki67+ nuclei was performed within the open-source ImageJ distribution Fiji (Schindelin et al., 2012) with a custom-made macro to obtain the number of total nuclei and Ki67+ nuclei, GFP area, and F-actin area from the acquired images (shown below):

```
Run ("Gaussian Blur…", "sigma=2 scaled stack");
SetAutoThreshold("IsoData dark");
//run("Threshold…");
setOption("BlackBackground", true);
run("Convert to Mask", "method=IsoData background=Dark calculate black");
run("Make Binary", "method=Default background=Default calculate black");
run("Close-", "stack");
run("Watershed", "stack");
run("Analyze Particles…", "size=100-1000000 show=Outlines display clear summarize
add stack";
```

All representative images were created using Adobe Photoshop CS6 (Adobe Inc.) and subjected uniformly to a Gaussian Blur of 0.5 pixels and contrast/brightness adjustments for display purposes only.

MTT Assay

Cells were transfected with wildtype AnkB or AnkB p.S646F-GFP plasmid, or treated with a toxic dose of 300 μg/mL cycloheximide (as a control for apoptosis) 24 h after plating in a 96 well plate. The MTT (3-(4,5-Dimetylthiazol-2-yl)-2,5-diphenyltetrazolium bromide) assay was performed 48 h post transfection/treatment as per the Vybrant MTT Cell Proliferation Assay

Kit 'Quick Protocol' (V1354; Invitrogen by ThermoFisher Scientific). Briefly, each well was replaced with 100 μL fresh media and incubated with 10 μL of the 12 mM MTT stock solution. After labelling, all but 25 μL of the culture medium was removed, 50 μL of DMSO was added, and the cells were incubated at 37 °C for 10 min. Absorbance was read at 540 nm (Infinite®200 PRO microplate reader, Tecan Life Sciences). All absorbance values were normalized to blank (vehicle control media, containing no cells). One N represents the average of 9 scans per well, and 8 wells were analyzed for each condition (N=8).

Trypan Blue Proliferation Assay

Cells were re-plated 24 h after transfection at a density of 355 cells/cm^2. Trypan Blue Dye (0.4% Trypan Blue in PBS; Stem Cell) was used as per manufacturer's protocol to count live and dead cells. The first cell count began 6 h after re-plating and every 24 h thereafter for a total of 5 timepoints.

Flow cytometry

Cells were plated at a density of 8,333 cells/cm^2 and transfected with either wildtype AnkB or AnkB p.S646F -GFP 24 h post-seeding. Cells were collected 48 h post-transfection using Versene (Gibco) and the cell suspension was transferred to a 96 well plate at 3 wells per sample and 3 samples per condition. Samples were analyzed using Guava easyCyte 5HT (Millipore).

Statistical Analysis

All results are represented as mean ± SEM. Statistical analysis was performed with Prism 7 for Mac OS X (Version 7.0a, GraphPad Software, Inc.) and is described in detail in each figure caption. Values for $p < 0.05$ were considered statistically significant.

RESULTS

The AnkB p.S646F variant increases AnkB targeting for proteasomal degradation in undifferentiated but not in differentiated H9c2 cells

In order to study how AnkB levels are regulated in cardiomyoblasts, we expressed wildtype AnkB in the H9c2 cardiomyoblast cell line. To distinguish between two primary pathways of protein degradation, wildtype AnkB-GFP expressing H9c2 cells were incubated with a proteasomal inhibitor, PS-341, or a lysosomal inhibitor, Bafilomycin A1 (BafA) (Fig. 1A). The level of expression of AnkB-GFP was determine by Western blotting using an anti-GFP antibody (Fig. 1Aii and iv). Treatment with PS-341 (25 nM or 50 nM) increased the expression level of wildtype AnkB relative to vehicle control (Fig. 1Aii). Incubation with the lysosomal inhibitor (10 nM and 25 nM BafA) did not significantly change the expression level of wildtype AnkB compared to vehicle control (Fig. 1Aiv). We also stripped and re-probed these membranes with anti-AnkB to look at the effect of PS-341 and BafA on endogenous AnkB (Fig. 1Aiii and v). Using anti-AnkB, PS-341 appeared to produce an even greater increase in AnkB. However, due to the large size of AnkB (220 kDa), it was not possible to resolve endogenous AnkB from exogenous AnkB-GFP, such that the signal reflects both endogenous and exogenous AnkB. These findings suggest the proteasome is responsible for wildtype AnkB degradation in H9c2 cells.

We then sought to determine if inhibition of the proteasome could rescue the reduced expression level of AnkB p.S646F (Fig. 1B). Consistent with our previous observations (Swayne et al. 2017), the expression level of AnkB p.S646F was significantly lower than that of wildtype AnkB (Fig. 1Bii). Treatment of AnkB p.S646F-GFP transfected H9c2 cells with 10 nM PS-341 elevated the expression level of AnkB p.S646F-GFP to that of wildtype AnkB (Fig. 1Bii).

Similarly, examination with anti-AnkB suggested that PS-341 significantly increased endogenous and exogenous AnkB in both wildtype AnkB and AnkB p.S646F transfected H9c2 (Fig. 1Biii). Therefore, the expression level of AnkB p.S646F can be rescued by inhibition of the proteasome.

To determine if proteasome inhibition has similar effects in differentiated H9c2 cells, cells were differentiated using low serum and RA (Menard et al. 1999; Branco et al. 2015). Notably, in the differentiated state, wildtype AnkB and AnkB p.S646F expression levels were not significantly different (Fig. 2). Moreover, when treated with PS-341, only wildtype AnkB significantly increased in expression levels, suggesting that PS-341 was unable to rescue AnkB p.S646F levels in differentiated H9c2.

AnkB p.S646F decreases cell viability

To determine the impact of AnkB p.S646F on cardiomyoblast growth, H9c2 cells were transfected with wildtype AnkB or AnkB p.S646F, and cells were counted every 24 h for 96 h in the presence of Trypan Blue (Fig. 3), which will only enter dead or dying cells whose plasma membrane is sufficiently compromised. Significantly lower numbers of live cells were observed in H9c2 cultures expressing AnkB p.S646F over time (Fig. 3A). Wildtype AnkB and AnkB p.S646F overexpression produced cell doubling times that were not significantly different (wildtype: 32.5 h, p.S646F: 30.3h; $P = 0.5755$ by t-test, N = 5), suggesting that this difference in live cell counts over time was not due to differences in cell proliferation. The percentage of dead cells in wildtype AnkB and AnkB p.S646F expressing cultures was plotted across time (Fig. 3B) revealing that 6 h after plating (30 h post-transfection), AnkB p.S646F expression was associated with ≈ 19% increase in the percentage of dead cells compared to wildtype AnkB (p.S646F: 41.3% ± 3.9; wildtype: 21.9% ± 3.9; $P < 0.0001$ Bonferroni's multiple comparison; Fig. 3B).

These results suggest decreased cell viability of AnkB p.S646F-expressing cells during the initial lag phase of cell growth.

To further investigate the impact of AnkB p.S646F expression on cell viability in H9c2 cells, we compared the metabolic activity of wildtype AnkB and AnkB p.S646F-expressing cells by MTT assay. A toxic dose of CHX (300 μg/mL), a protein translation inhibitor (Alvarez-Castelao et al. 2012), served as a positive control for cells with compromised metabolic activity and viability. H9c2 cells expressing AnkB p.S646F exhibited a small but significant reduction in metabolic activity (Fig. 4). These results support the results of the Trypan Blue assay (Fig. 3), suggesting that expression of AnkB p.S646F impairs cell viability.

Confocal fluorescence microscopy revealed that both wildtype AnkB and AnkB p.S646F localized to the membrane and intracellular compartments as shown by the close association of the GFP and anti-AnkB signals with WGA (Fig. 5A). Additionally, we immunostained transfected H9c2 cells with Ki67, which is a marker of proliferating cells (Gerdes et al. 1984) (Fig. 5B). Notably, AnkB p.S646F transfected H9c2 cultures exhibited a higher proportion of Ki67-positive cells (Fig. 5Ci). We also compared cell size between wildtype AnkB and AnkB p.S646F transfected H9c2 cultures using total actin area normalized to the number of nuclei within the same field-of-view and found no significant differences (Fig. 5Cii). It is important to note that we detected the presence of double nuclei in both wildtype AnkB and AnkB p.S646F cultures, although there were no obvious differences between genotypes (albeit not quantified). Only a small proportion of H9c2 cells were GFP-positive (wildtype AnkB-GFP 4.9 %; AnkB p.S646F-GFP 5.5%).

AnkB p.S646F expresses at lower levels in individual undifferentiated H9c2 cells

To ensure that the lower AnkB p.S646F expression levels seen in untreated H9c2 cells (Fig. 1B) were not simply caused by selective loss of AnkB p.S646F expressing cells (with concomitant expansion of non-expressing cells), we also measured GFP fluorescence intensity of individual cells using flow cytometry. We observed a shift towards lower fluorescence intensity in cells transfected with AnkB p.S646F compared with wildtype AnkB expressing cells (Fig. 6A). The mean fluorescence intensity of AnkB p.S646F-expressing cells was also significantly lower than wildtype, confirming that on a cellular level, AnkB p.S646F is expressed at lower levels than wildtype AnkB (wildtype: 9.5 a.u., p.S646F: 6.0 a.u.; $P = 0.0011$ by t-test, N = 3; Fig. 4B).

DISCUSSION

The role of AnkB in the proteostasis of its binding partners in the cardiomyocyte is well established (Mohler et al. 2005; Cunha et al. 2007), but our understanding of the proteostasis of AnkB itself is limited. This is critically important for understanding its role in cardiomyocyte biology. Here we investigated the mechanism of AnkB degradation as well as the impact of a novel variant AnkB p.S646F on this process, and on cell viability in H9c2 rat ventricular cardiomyoblast cells.

We recently showed that AnkB p.S646F is unique in the context of other disease-causing AnkB variants, in that it effects AnkB stability (Swayne et al. 2017). Other variants did not exhibit decreased protein levels when exogenously expressed in cardiomyocytes (Mohler et al. 2007b). Here we found that inhibition of the proteasome led to expression of AnkB p.S646F at levels similar to those of wildtype AnkB in H9c2 cells, suggesting that the p.S646F mutation causes AnkB to become targeted for proteasomal degradation. Although we were unable to

differentiate endogenous AnkB from exogenous AnkB p.S646F-GFP, wildtype AnkB and AnkB p.S646F transfected H9c2 cells exhibited no significant differences with anti-AnkB (reflecting signal from both endogenous and ectopic AnkB), suggesting AnkB p.S646F does trigger degradation of wildtype AnkB. These findings suggest that the cellular pathology resulting from expression of AnkB p.S646F variant is due to protein dysfunction rather than directly affecting wildtype AnkB stability. In terms of the underlying mechanism of increased AnkB p.S646F proteasomal degradation in the context of immature, undifferentiated H9c2 cells, addition of the hydrophobic phenylalanine residue and resulting tertiary (or quaternary) structural changes could enhance the likelihood of AnkB p.S646F ubiquitination (Schröder and Kaufman 2005; Hetz et al. 2011; Oikawa et al. 2012). In our previous report, the folding of the purified MBD with the p.S646F mutation was similar to that of the wildtype MBD (Swayne et al. 2017), suggesting there was no inherent instability within the MBD caused by the mutation. However, the MBD has previously been shown to participate in intramolecular interactions with the C-terminal domain (Abdi et al. 2006), such that the p.S646F mutation could affect intramolecular interactions of the MBD with the C-terminal domain, or intermolecular interactions with post-translational modification machinery or proteins, resulting in relative instability within cells. Resulting from these aberrant intra- or inter-molecular interactions, the p.S646F mutation could increase the association of AnkB p.S646F with E3 ubiquitin ligases to facilitate AnkB degradation. Precisely how AnkB p.S646F leads to increased proteasome degradation will be the focus of future work.

Our characterization of cellular behaviours in wildtype AnkB and AnkB p.S646F expressing H9c2 cells suggest a complex, time-dependent effect on viability and proliferation (Fig. 7). AnkB p.S646F expression led to an increased number of compromised cells, analyzed

by trypan blue exclusion at 30 h post-transfection and MTT assay at 48 h post-transfection. Additionally, we observed an increased proportion of actively cycle 48 h post-transfection as indicated by Ki67 immunoreactivity. Although we used Ki67 as a binary indicator of cycling cells in our analysis, it should be noted, that recent work suggests Ki67 exhibits a graded response, influenced not only by the cycle stage, but also the cell type and length of time in arrest before re-entering cell cycle (Miller et al. 2018). Future in-depth examination of Ki67 localization and intensity could serve to better understand the impact of AnkB and AnkB variants on H9c2 cell cycle dynamics. Notably, both wildtype AnkB and AnkB p.S646F-expressing cultures exhibited similar, low numbers of GFP-positive cells at 48 h post-transfection, suggesting that the observed differences in viability and proliferation were not due to selective loss of transfected cells, but rather a population effect via paracrine communication. Cardiomyocytes are known to release "cardiokines" when under stress (as reviewed in Dewey et al. 2016). These cardiokines can impact proliferation, differentiation, and inflammation, and can have both beneficial and detrimental effects, inhibiting and promoting apoptosis (as reviewed in Wu et al. 2018). Future work will examine the potential role for AnkB in regulating paracrine communication in H9c2 cells and cardiomyocytes. Additionally, given AnkB's role as a scaffold protein for several ion channels and receptors involved in regulating intracellular Ca^{2+} homeostasis, AnkB is like to be involved in the regulation of cellular viability. The Ca^{2+} dependence of key cell death/survival-regulating proteins is well-known (as reviewed in Zhivotovsky and Orrenius 2011). Moreover, Ca^{2+} also acts as an important factor in cellular development by regulating Ca^{2+}-dependent gene expression mechanisms (Sheng et al. 1991; West et al. 2001; Hogan et al. 2003) raising the possibility that AnkB could similarly play a role in cardiomyocyte development. Our results showing AnkB p.S646F was less stable only in

undifferentiated H9c2 cells suggest the impact of the p.S646F variant occurs during cellular development and thus could impact on the overall structural and functional development of the heart. Ultimately, the impact of AnkB p.S646F on AnkB stability and H9c2 cell survival provides additional insight into the potential etiology of cardiac dysfunction observed in patients.

Author contributions

LC conducted the degradation, proteasome and lysosome inhibition, and MTT assay experiments. LC performed the cell culture work for the proliferation assay, and jointly counted cells with CSWC. CSWC performed flow cytometry and differentiated proteasome and lysosome inhibition. JCSA performed confocal imaging and analysis. LC and CSWC analyzed data and created figures. LAS, LC, CSWC, JCSA and LA wrote and edited the manuscript. The authors declare no competing interests.

Acknowledgements

LC was supported by a Natural Sciences and Engineering Research Council of Canada CGS-M and University of Victoria graduate scholarships. LAS is supported by the Michael Smith Foundation for Health Research & BC Schizophrenia Society Foundation Scholar award. This research was funded by the University of Victoria seed funds to LAS, and CIHR funding (PJT-153392) awarded to LTA and LAS. We acknowledge that this research was conducted on the Indigenous traditional territory of the W̲SÁNEĆ, Lkwungen, and Wyomilth peoples of the Coast Salish Nation, and appreciate the continued partnership with the Gitxsan peoples and the Gitxsan Health Society in their research priorities.

REFERENCES

Abdi, K.M., Mohler, P.J., Davis, J.Q., and Bennett, V. 2006. Isoform specificity of ankyrin-B: A site in the divergent C-terminal domain is required for intramolecular association. J. Biol. Chem. **281**(9): 5741–5749. doi:10.1074/jbc.M506697200.

Alvarez-Castelao, B., Ruiz-Rivas, C., and Castaño, J.G. 2012. A critical appraisal of quantitative studies of protein degradation in the framework of cellular proteostasis. Biochem. Res. Int. **2012**. doi:10.1155/2012/823597.

Branco, A.F., Pereira, S.P., Gonzalez, S., Gusev, O., Rizvanov, A.A., and Oliveira, P.J. 2015. Gene Expression Profiling of H9c2 Myoblast Differentiation towards a Cardiac-Like Phenotype. PLoS One **10**(6): e0129303. doi:10.1371/journal.pone.0129303.

Cunha, S.R., Bhasin, N., and Mohler, P.J. 2007. Targeting and stability of Na/Ca exchanger 1 in cardiomyocytes requires direct interaction with the membrane adaptor ankyrin-B. J. Biol. Chem. **282**(7): 4875–4883. doi:10.1074/jbc.M607096200.

Dewey, C.M., Spitler, K.M., Ponce, J.M., Hall, D.D., and Grueter, C.E. 2016. Cardiac-secreted factors as peripheral metabolic regulators and potential disease biomarkers. J. Am. Heart Assoc. **5**(6): 1–14. doi:10.1161/JAHA.115.003101.

Gerdes, J., Lemke, H., Baisch, H., Wacker, H., Schwab, U., and Stein, H. 1984. Cell cycle analysis of a cell proliferation-associated human nuclear antigen defined by the monoclonal antibody Why The JI ? Submit online . • Rapid Reviews ! 30 days * from submission to initial decision • No Triage ! Every submission reviewed by practic. J. Immunol. **133**(4): 1710–1715.

Hetz, C., Martinon, F., Rodriguez, D., and Glimcher, L.H. 2011. The unfolded protein response: integrating stress signals through the stress sensor IRE1α. Physiol. Rev. **91**(4): 1219–43.

doi:10.1152/physrev.00001.2011.

Hogan, P.G., Chen, L., Nardone, J., and Rao, A. 2003. Transcriptional regulation by calcium, calcineurin, and NFAT. doi:10.1101/gad.1102703.

Koenig, S.N., and Mohler, P.J. 2017. The evolving role of ankyrin-B in cardiovascular disease. Hear. Rhythm **14**(12): 1884–1889. Elsevier. doi:10.1016/J.HRTHM.2017.07.032.

Menard, C., Pupier, S., Mornet, D., Kitzmann, M., Nargeot, J., and Lory, P. 1999. Modulation of L-type calcium channel expression during retinoic acid- induced differentiation of H9C2 cardiac cells. J. Biol. Chem. **274**(0021–9258 SB–IM): 29063–29070.

Miller, I., Min, M., Yang, C., Tian, C., Gookin, S., Carter, D., and Spencer, S.L. 2018. Ki67 is a Graded Rather than a Binary Marker of Proliferation versus Quiescence. Cell Rep. **24**(5): 1105–1112.e5. ElsevierCompany. doi:10.1016/j.celrep.2018.06.110.

Mohler, P.J., Davis, J.Q., and Bennett, V. 2005. Ankyrin-B coordinates the Na/K ATPase, Na/Ca exchanger, and InsP3 receptor in a cardiac T-tubule/SR microdomain. PLoS Biol. **3**(12): 2158–2167. doi:10.1371/journal.pbio.0030423.

Mohler, P.J., Gramolini, A.O., and Bennett, V. 2002. The ankyrin-B C-terminal domain determines activity of ankyrin-B/G chimeras in rescue of abnormal inositol 1,4,5-trisphosphate and ryanodine receptor distribution in ankyrin-B (-/-) neonatal cardiomyocytes. J. Biol. Chem. **277**(12): 10599–10607. doi:10.1074/jbc.M110958200.

Mohler, P.J., Healy, J.A., Xue, H., Puca, A.A., Kline, C.F., Allingham, R.R., Kranias, E.G., Rockman, H.A., and Bennett, V. 2007a. Ankyrin-B syndrome: enhanced cardiac function balanced by risk of cardiac death and premature senescence. PLoS One **2**(10): e1051. doi:10.1371/journal.pone.0001051.

Mohler, P.J., Schott, J.-J., Gramolini, a O., Dilly, K.W., Guatimoisim, S., DuBell, W.H., Song,

L.-S., Haurogne, K., Kyndt, F., Ali, M.E., Rogers, T.B., Lederer, W.J., Escande, D., Marec, H. Le, and Bennett, V. 2003. Ankyrin-B mutations causes type 4 long-QT cardiac arrhythmia and sudden cardiac death. Nature **421**: 634–639. doi:10.1038/nature01384.1.

Mohler, P.J., Le Scouarnec, S., Denjoy, I., Lowe, J.S., Guicheney, P., Caron, L., Driskell, I.M., Schott, J.-J., Norris, K., Leenhardt, A., Kim, R.B., Escande, D., and Roden, D.M. 2007b. Defining the Cellular Phenotype of "Ankyrin-B Syndrome" Variants. Circulation **115**(4). doi:10.1161/CIRCULATIONAHA.106.656512.

Mohler, P.J., Splawski, I., Napolitano, C., Bottelli, G., Sharpe, L., Timothy, K., Priori, S.G., Keating, M.T., and Bennett, V. 2004. A cardiac arrhythmia syndrome caused by loss of ankyrin-B function. Proc. Natl. Acad. Sci. U. S. A. **101**(24): 9137–42. doi:10.1073/pnas.0402546101.

Oikawa, D., Kitamura, A., Kinjo, M., and Iwawaki, T. 2012. Direct association of unfolded proteins with mammalian ER stress sensor, IRE1β. PLoS One **7**(12): e51290. doi:10.1371/journal.pone.0051290.

El Refaey, M.M., and Mohler, P.J. 2017. Ankyrins and Spectrins in Cardiovascular Biology and Disease. Front. Physiol. **8**: 852. Frontiers. doi:10.3389/fphys.2017.00852.

Schneider, C.A., Rasband, W.S., and Eliceiri, K.W. 2012. NIH Image to ImageJ: 25 years of image analysis. Nat. Methods. doi:10.1038/nmeth.2089.

Schröder, M., and Kaufman, R.J. 2005. The mammalian unfolded protein response. Annu. Rev. Biochem. **74**: 739–89. doi:10.1146/annurev.biochem.73.011303.074134.

Scotland, P., Zhou, D., Benveniste, H., and Bennett, V. 1998. Nervous system defects of AnkyrinB(-/-) mice suggest functional overlap between the cell adhesion molecule L1 and 440-kD AnkyrinB in premyelinated axons. J. Cell Biol. **143**(5): 1305–1315.

401 doi:10.1083/jcb.143.5.1305.
402 Sheng, M., Thompson, M.A., and Greenberg, M.E. 1991. CREB: A Ca2+-regulated transcription
403 factor phosphorylated by calmodulin-dependent kinases. Science (80-.).
404 doi:10.1126/science.1646483.
405 Swayne, L.A., Murphy, N.P., Asuri, S., Chen, L., Xu, X., McIntosh, S., Wang, C., Lancione,
406 P.J., Roberts, J.D., Kerr, C., Sanatani, S., Sherwin, E., Kline, C.F., Zhang, M., Mohler, P.J.,
407 and Arbour, L.T. 2017. Novel variant in the ANK2 membrane-binding domain is associated
408 with Ankyrin-B syndrome and structural heart disease in a first nations population with a
409 high rate of long QT syndrome. Circ. Cardiovasc. Genet. **10**: e001537.
410 doi:10.1161/CIRCGENETICS.116.001537.
411 West, A.E., Chen, W.G., Dalva, M.B., Dolmetsch, R.E., Kornhauser, J.M., Shaywitz, A.J.,
412 Takasu, M.A., Tao, X., and Greenberg, M.E. 2001. Calcium regulation of neuronal gene
413 expression. Proc. Natl. Acad. Sci. doi:10.1073/pnas.191352298.
414 Wu, Y.S., Zhu, B., Luo, A.L., Yang, L., and Yang, C. 2018. The role of cardiokines in heart
415 diseases: Beneficial or detrimental? Biomed Res. Int. **2018**. Hindawi.
416 doi:10.1155/2018/8207058.
417 Zhivotovsky, B., and Orrenius, S. 2011. Calcium and cell death mechanisms: A perspective from
418 the cell death community. doi:10.1016/j.ceca.2011.03.003.
419

FIGURE CAPTIONS

Fig. 1. Proteasome inhibition partially rescues AnkB p.S646F expression levels. Ai. Western blot of wildtype-AnkB-GFP-expressing H9c2 cells treated with proteasomal inhibitor, PS-341, or lysosomal inhibitor, Bafilomycin A, BafA, at the indicated concentrations for 12 h. Western blots were probed for anti-GFP, anti-AnkB, or anti-β-actin. **Aii.** Histogram of GFP levels assessed by Western blotting normalized to β-actin immunoreactivity and expressed as % control with PS-341 treatment. One way ANOVA: $P = 0.0003$ by one-way ANOVA, (***) $P = 0.0005$ by Dunnett's multiple comparison; N = 3. **Aiii.** Histogram of AnkB levels assessed by Western blotting normalized to β-actin immunoreactivity and expressed as % control with PS-341 treatment. One way ANOVA: $P < 0.0001$ by one-way ANOVA, (****) $P < 0.0001$ by Dunnett's multiple comparison; N = 3. **Aiv.** Histogram of GFP levels assessed by Western blotting normalized to β-actin immunoreactivity and expressed as % control with BafA treatment. One way ANOVA: $P = 0.1650$ by one-way ANOVA; N = 3. **Av.** Histogram of AnkB levels assessed by Western blotting normalized to β-actin immunoreactivity and expressed as % control with BafA treatment. One way ANOVA: $P = 0.0088$ by one-way ANOVA, (n.s.) $P = 0.5294$ (10 nM), (**) $P = 0.0068$ (25 nM) by Dunnett's multiple comparison; N = 3. **Bi.** Western blot of wildtype AnkB or AnkB p.S646F -GFP expressing H9c2 cells treated with 0 nM or 10 nM PS-341 probed with anti-GFP, anti-AnkB, or anti β-actin. **Bii.** Histogram of GFP levels assessed by Western blotting normalized to β-actin immunoreactivity and expressed as % control. Two-way ANOVA: Genotype: $F_{(1,8)} = 14.32$, $P = 0.0054$; Treatment: $F_{(1,8)} = 24.48$, $P = 0.0011$; Interaction: $F_{(1,8)} = 0.4887$, $P = 0.5043$; Sidak's multiple comparison (*) $P = 0.0262$ (DMSO: WT vs S6464F), (n.s.) P = 0.1177 (PS-341: WT vs S646F); N=3. **Biii.** Histogram of AnkB levels assessed by Western

443 blotting normalized to β-actin immunoreactivity and expressed as % control. Two-way ANOVA:
444 Genotype: $F_{(1,8)} = 3.410$, $P = 0.1020$; Treatment: $F_{(1,8)} = 60.42$, $P < 0.0001$; Interaction: $F_{(1,8)} =$
445 1.710, $P = 0.2273$; Sidak's multiple comparison (n.s.) $P = 0.1093$ (DMSO: WT vs S646F), (n.s.)
446 $P = 0.9176$ (PS-341: WT vs S646F); N=3. These data are included in the MSc thesis of Lena
447 Chen found at: https://dspace.library.uvic.ca/handle/1828/9346.
448
449 **Fig. 2. Wildtype AnkB and AnkB p.S646F is similarly expressed in differentiated H9c2**
450 **cells.** Western blot of wildtype AnkB or AnkB p.S646F -GFP expressing H9c2 cells treated with
451 0 nM or 10 nM PS-341 probed with anti-GFP or anti β-actin. **Bii.** Histogram of GFP levels
452 assessed by Western blotting normalized to β-actin immunoreactivity and expressed as %
453 control. Two-way ANOVA: Genotype: $F_{(1,8)} = 2.508$, $P = 0.1519$; Treatment: $F_{(1,8)} = 9.996$, $P =$
454 0.0134; Interaction: $F_{(1,8)} = 9.718$, $P = 0.0143$; Sidak's multiple comparison (n.s.) $P = 0.5235$
455 (DMSO: WT vs S646F), (*) $P = 0.0208$ (PS-341: WT vs S646F); N=3.
456
457 **Fig. 3. AnkB p.S646F results in an early reduction in cell viability.** Growth curve of AnkB
458 and AnkB p.S646F -GFP expressing H9c2 cells. Live and dead cells were counted with Trypan
459 Blue 6 h after re-plating (0 h; equivalent to 30 h post-transfection), and every 24 h for 96 h in
460 total. **A.** Mean live cell numbers (x 10^4) across time. There was a significant difference in the
461 number of live AnkB p.S646F-expressing H9c2 cells and wildtype AnkB-expressing cells across
462 time. Two-way ANOVA: $F_{(1,40)} = 6.035$, $P = 0.0185$; Time: $F_{(4,40)} = 81.86$, $P < 0.0001$;
463 Interaction $F_{(4,40)} = 0.5959$ $P = 0.6676$ by two-way ANOVA; Bonferroni's multiple comparisons
464 indicate $P > 0.05$ between wildtype and AnkB p.S646F for all time points; N = 5). Doubling time
465 for wildtype live cells and AnkB p.S646F live cells were similar at 32.5 h and 30.3 h,

466 respectively. **B.** Mean dead cell number as a % total cell number for wildtype and AnkB p.S646F
467 cultures**.** Two-way ANOVA: Genotype: $F_{(1,40)} = 9.516$, $P = 0.0037$; Time: $F_{(4,40)} = 19.33$, $P <$
468 0.0001, Interaction: $F_{(4,40)} = 5.197$, $P = 0.0018$ by; Bonferroni's multiple comparison (****) $P <$
469 0.0001; N = 5. These data are included in the MSc thesis of Lena Chen found at:
470 https://dspace.library.uvic.ca/handle/1828/9346.
471
472 **Fig. 4. AnkB p.S646F reduces metabolic activity.** MTT (3-(4,5-Dimethylthiazol-2-yl)-3,5-
473 diphenyltetrazolium bromide) assay for metabolic activity conducted 48 h post-transfection with
474 wildtype AnkB or AnkB p.S646F-GFP expressing H9c2 cells. A toxic dose of cycloheximide
475 (300 µg/mL ;10X CHX) served as a negative control for cell viability. All data are normalized to
476 blanks (MTT solution in cell culture media alone), and presented as % untransfected control.
477 One-way ANOVA: $P < 0.0001$, (**) $P = 0.0019$ and (****) $P < 0.0001$ by Bonferroni's multiple
478 comparisons; N = 8. These data are included in the MSc thesis of Lena Chen found at:
479 https://dspace.library.uvic.ca/handle/1828/9346.
480
481 **Fig. 5. AnkB p.S646F has higher proportion of cells with Ki67. A.** Wildtype AnkB and AnkB
482 p.S646F localize to the membrane and intracellular compartments. Representative optical
483 sections of H9c2 transfected with wildtype AnkB and AnkB p.S646F and labeled with anti-
484 AnkB and WGA. The GFP and anti-AnkB fluorescence signals distributed along the membrane
485 and intracellular compartments for wildtype AnkB and AnkB p.S646F. Scale bar, 10 µm. B**.**
486 Representative images of wildtype AnkB and AnkB p.S646F -GFP expressing H9c2cells, stained
487 with anti-Ki67 and phalloidin (F-actin). Scale bar 500 µm. **Ci.** Quantification of Ki67-positive
488 cells per total number of cells as a percentage of wildtype. AnkB p.S646F had higher number of

cells with Ki67. T-test: (*) $P = 0.0230$; N = 3. C**ii.** Quantification of area based on actin per total number of cells as percentage of wildtype. T-test: (n.s.) $P = 0.1405$; N = 3.

Fig. 6. AnkB p.S646F expresses at lower levels in individual H9c2 cells. Results of flow cytometry analysis conducted 48 h post-transfection with wildtype AnkB or AnkB p.S646F -GFP in H9c2 cells. **A.** Histogram of H9c2 transfected with wildtype AnkB or AnkB p.S646F -GFP. The distribution of GFP signal in AnkB p.S646F-GFP expressing cells appears to be shifted towards lower fluorescence intensity. **B.** Histogram of mean GFP fluorescent intensity of wildtype-AnkB and AnkB p.S646F -GFP expressing cells. GFP mean fluorescent intensity was significantly lower in AnkB p.S646F-GFP-expressing cells than wildtype AnkB-expressing cells. T-test: (**) $P = 0.0011$; N = 3.

Fig. 7. Timeline of AnkB p.S646F effects on H9c2 cardiomyoblasts. Expression of AnkB p.S646F in H9c2 cells decreased their viability and also increased cell proliferation at different times following transfection.

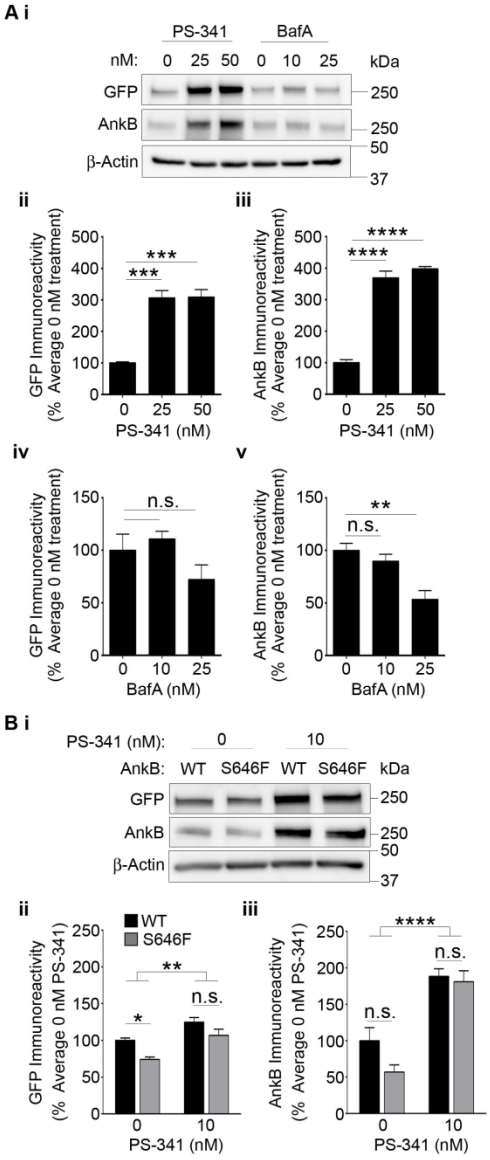

Figure 1

177x254mm (300 x 300 DPI)

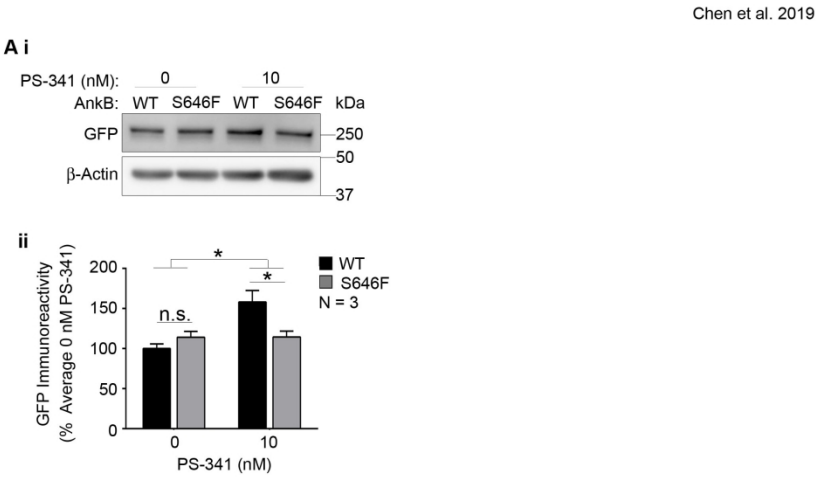

Figure 2

177x254mm (300 x 300 DPI)

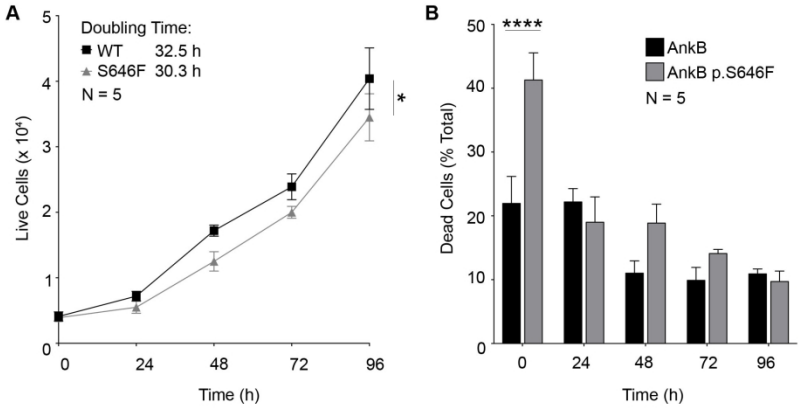

Figure 3

177x254mm (300 x 300 DPI)

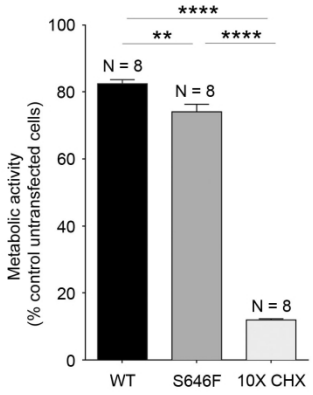

Figure 4

177x254mm (300 x 300 DPI)

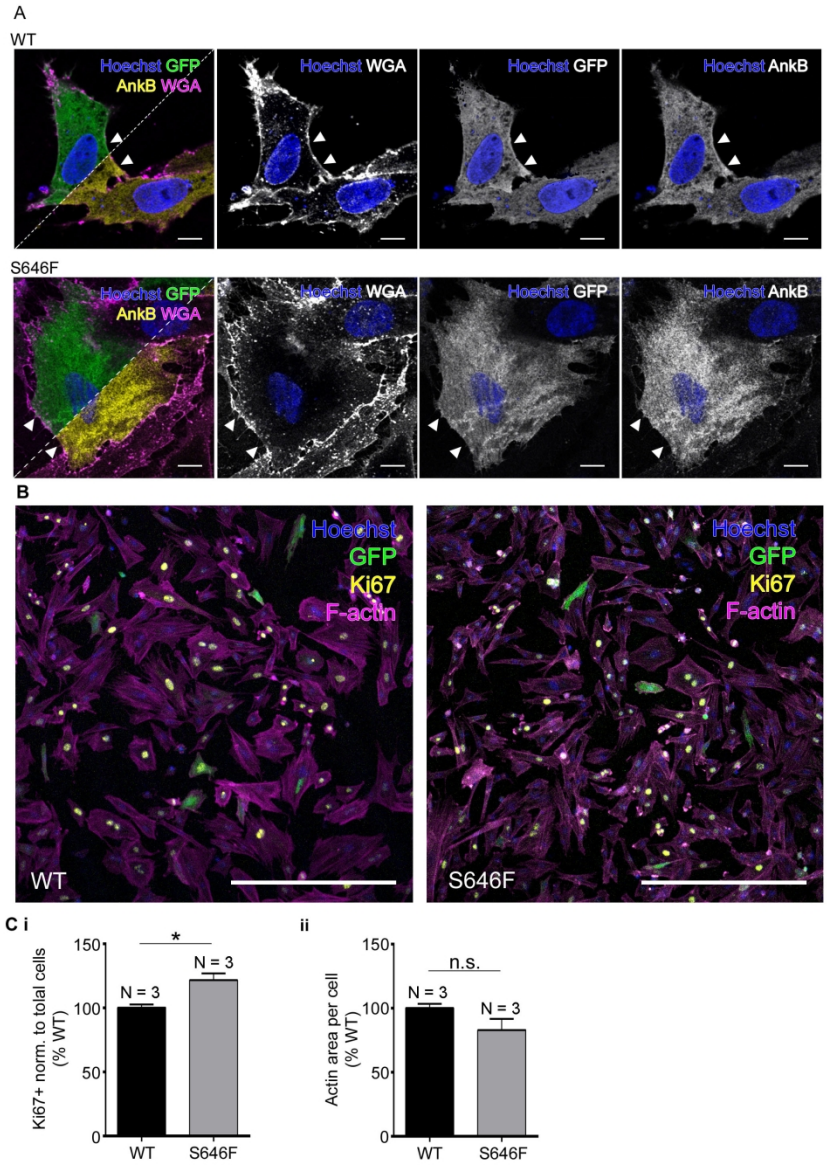

Figure 5

177x254mm (300 x 300 DPI)

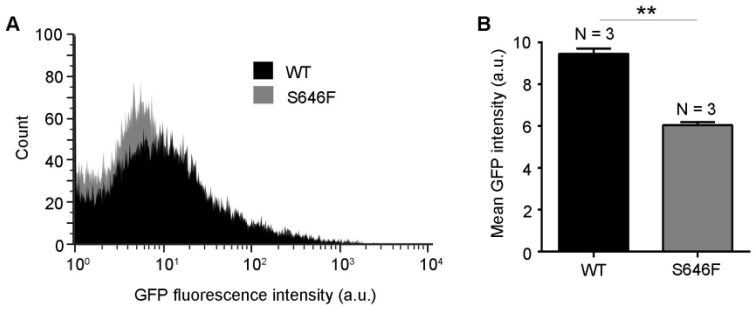

Figure 6

177x254mm (300 x 300 DPI)

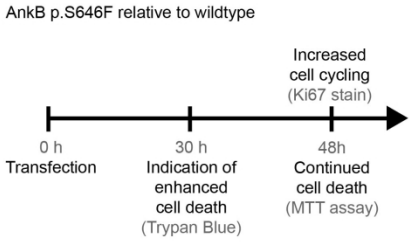

Figure 7

177x254mm (300 x 300 DPI)